# A Machine Learning Approach for Discovering and Engineering Bulk Metallic Glass Alloys


## Abstract

Bulk metallic glasses (BMGs) are an exciting, commercially-important class of materials that possess a unique set of properties typical for both metallic and amorphous materials. For example, BMGs feature fracture toughnesses comparable to crystalline metals and yield strengths twice as large as titanium alloys, but can be processed using techniques conventionally reserved for plastics, such as blow molding. These properties make them interesting materials for a number of applications, including biomedical implants. However, metallic glasses are only possible to form at special compositions that have proven extremely challenging to locate. Even when a new metallic glass is found, it is difficult to optimize the composition of a material to tune its properties for a specific application. Solving these problems is complicated by the lack of a computational modelling approach for linking the composition of a BMG to its properties. To address this issue, we approached the design of metallic glasses with data analytics.

In this report, we describe a framework for designing metallic glasses using several models developed using machine learning. These models were created with metallic glass data collected entirely from the publically-available literature. We used machine learning to identify how factors derived from the composition of an alloy are linked to its ability to form a metallic glass, critical casting thickness ($D_{max}$), and supercooled liquid range ($\Delta T_x$). We find that these models have high predictive accuracy in cross-validation and are capable of accurately predicting properties in yet-unassessed alloy systems.

We also employed the models for two different design tasks: (1) identifying new metallic glass alloys, and (2) optimizing the properties of known alloys to maximize casting thickness and $\Delta T_x$. To date, we have tested the performance of several predicted alloys using commercial processing techniques. We have been able to locate alloys with improved properties in one of our two design variables, $\Delta T_x$, by tuning existing alloys. Experiments to find BMGs in new alloy systems are ongoing. We envision that this technology will enable tailoring bulk metallic glass alloys for new applications, which will make it easier to utilize their superior properties for a variety of technologies.

## Graphical Abstract

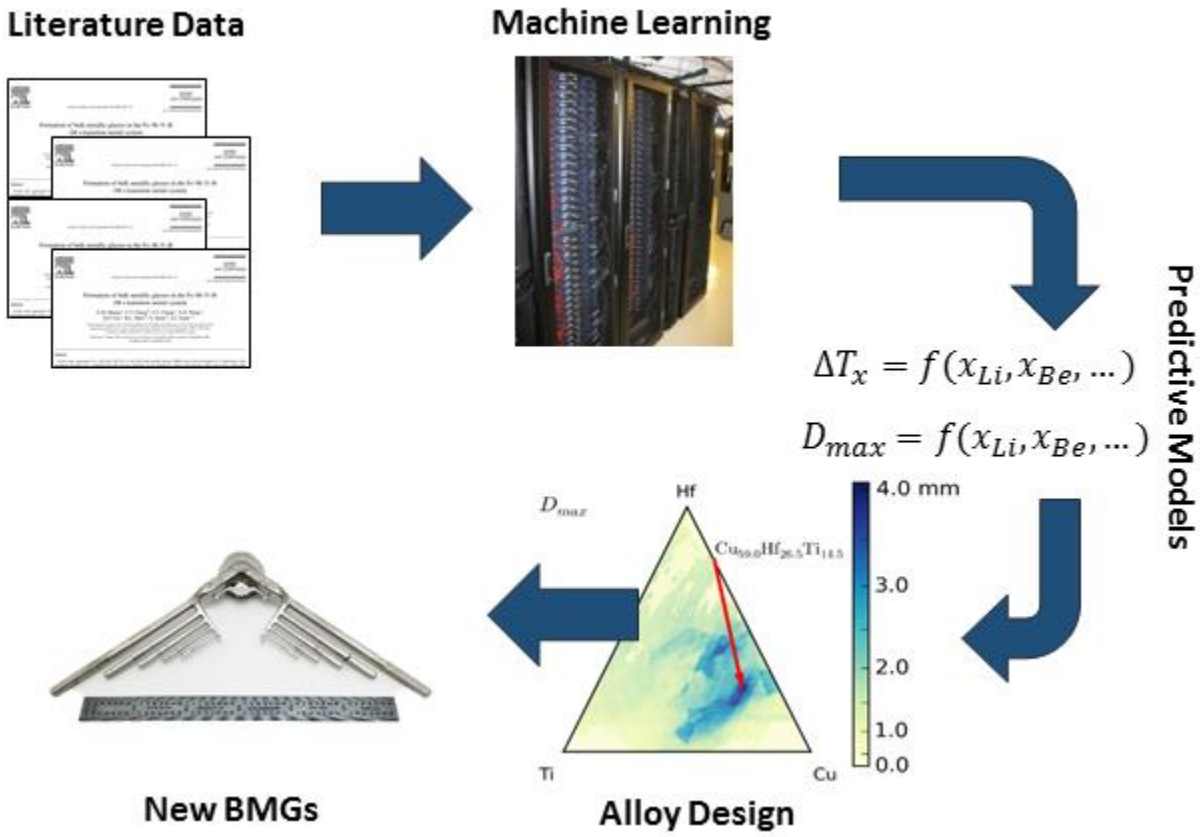


## Statement of Significance

Bulk Metallic Glasses (BMGs) are unique materials that combine properties of metal alloys and ceramic glasses. However useful, it is difficult to locate alloys that can form as glasses and to optimize known alloys for new applications. Engineering BMGs is complicated by the lack of physics-based models for many key properties. Searches for new alloys are conventionally guided by empirical rules, with some success, but the process of designing alloys often requires significant experimental effort. In this report, we outline a machine-learning-based approach for designing BMGs using models created from data from the literature. This framework can be used to develop alloys that can be used for applications including wear-resistant medical implants and automotive parts.

## Background

While the amorphous structure of Bulk Metallic Glasses (BMGs) gives them properties that are impossible in conventional metallic alloys, it also makes them difficult to engineer. The lack of atomic-scale order leads to properties including high mechanical strength, low magnetic hysteresis, and the ability to be formed using net-shape casting techniques. These unique set of properties make them promising materials for applications such as surgical devices, biomedical implants, pressure sensors, mission critical flight control surfaces, sporting arms, automotive components, and more. However, owing to the energetic metastability of the amorphous structure, BMGs require special casting techniques to cool them fast enough to prevent crystallization. Additionally, only certain alloys are possible to form in the amorphous state and it is difficult to locate the composition of these alloys *a priori*. What would enable the wider-scale technological use of metallic glasses is the ability to locate new alloy compositions that can be fabricated using commercially-viable processing techniques.

Conventional alloy design for metallic glasses relies on empirical rules and extensive experimentation. For example, it is known that BMGs tend to form in systems with a large diversity in atomic sizes,[1] or near eutectic compositions.[2] These empirical rules can also be informed using physics-based models (e.g., computational thermodynamics to predict driving force for crystallization),[3–11] which often require both large computational resources and experimental measurements from each alloy system being assessed. However, even with the availability of these rules, extensive experimentation is often required to locate alloys with optimized properties.[12] Furthermore, there are some important properties (ex: supercooled liquid range), for which neither empirical rules nor physical models linking the composition and properties of the material exist. Fortunately, the fact that there are known empirical rules for metallic glass formation and large resources of experimental data available make a new tool for alloy design feasible: machine learning.

In this report, we will describe a machine learning framework for accelerating the design and discovery bulk metallic glasses that can be casted using state-of-the-art, commercial casting equipment. To do so, we used machine learning to create models for three key properties: the ability to form a metallic glass, critical casting thickness, and supercooled liquid range. These models were created with only data from the publically-available literature, and were designed to incorporate empirical rules about metallic glass formation. We then employed these models to suggest compositions of alloys that could have both large critical casting diameters and supercooled liquid ranges. If successful, these tools would enable the development of new, cheaper metallic glasses and the ability for engineers to tailor the properties of BMGs for specific applications. These capabilities would help accelerate the incorporation of a whole new class of materials into a wide variety of technologies.

## Methods

### Data Mining

Machine learning models are composed of three separate components: a resource of training data, a representation to describe key characteristics of each entry, and a machine learning algorithm. We will describe these three components separately.

## Training Data

Our training set was assembled from publically-available data collected from many different articles and handbooks. The data collection process was significantly aided by previous efforts in collecting large resources of metallic glass data, such as the Landolt-Bornstein Handbook on "Nonequilibrium Phase Diagrams of Ternary Amorphous Alloys"[13] and papers by Long *et al.*[14] and Tripathi *et al.*[15] A full list of the data collected and the papers from which it was extracted is provided along with this report. The data we collected was partitioned into three distinct training sets: a dataset of whether it was possible to create a bulk metallic glass, critical casting thicknesses, and supercooled liquid ranges.

### *Glass-Forming Ability Classification Dataset*

Our glass-forming ability training set was composed of 6315 measurements of whether it was reported to be possible to form a BMG, an amorphous ribbon via melt spinning, or not at all. This dataset was assembled by combining measurements of whether it was possible to form a glass with melt spinning, taken from the Landolt-Bornstein Handbook, with the compositions of known BMGs collected from 42 different papers. Where conflicting reports exist about the glass-forming ability of a certain composition, we select the most optimistic report (i.e., BMG over Ribbon over None) for inclusion within our dataset.

The entries in our dataset span a broad range of chemistries. As shown in Figure 1, the dataset contains 55 different elements, including transition metals and metalloids, and nearly all of these elements are present in examples of BMGs. Furthermore, the dataset includes examples of interactions between 513 pairs of elements, spanning metal/metal and metal/metalloid glasses.

There are two major biases in our data that need to be considered when training models. First of all, the only negative examples of glass-formation are from Ref. 13, which only contains alloys with 3 or fewer elements. Consequently, the number of elements in an alloy should not be used as a factor in our classification models. Additionally, as the ability to form a bulk glass was not tested during the ribbon forming experiments, a positive measurement of ribbon forming ability does not prove a material cannot be formed using bulk techniques. This issue limits the ability of our models to distinguish between bulk and ribbon-forming glasses, but not the ability to distinguish between glass-forming and non-glass-forming compositions.

### *Critical Casting Diameter Dataset*

The critical casting diameter ($D_{max}$) defines the largest thickness at which it is possible to cast a fully-amorphous rod of metallic glass. Our training dataset was created using the same source of literature as the classification dataset, and totals 5916 entries. For alloys extracted from the BMG literature, we used the value of critical casting diameter reported in the paper, if available. For alloys that were classified as ribbon-forming in the Landolt-Bornstein handbook,[13] we assumed a single, small value of 0.2 mm for the critical casting diameter of each alloy. Any alloy classified as "not glass-forming" was assigned a diameter of 0. When multiple values of the critical diameter were available, we used the average of all available measurements.

### *Supercooled Liquid Range Dataset*

The supercooled liquid range ($\Delta T_x$) is defined as the difference between the glass transition temperature ($T_g$) and temperature at which an alloy crystallizes on heating ($T_x$), and is correlated

with how easy a metallic glass can be shaped after solidification. Our training dataset is the smallest of the three at 621 entries, and includes 45 different elements and 307 different pairs (see Figure 1). Because $\Delta T_x$ measurements can vary significant for single alloys (ex: reports of $Y_6Fe_{77}B_{22}$ vary by 40 K[16,17]), we use the average of all measurements for a particular composition.

### Representation: Attributes to Describe Materials

The goal in selecting a representation for materials is to construct a set of numerical attributes that both differentiate materials and captures factors that could be related to the properties of interest. As our objective is to find new alloy compositions for BMGs, we chose to differentiate materials based on composition. To create factors derived from the composition that reflect empirical knowledge about glass-formation, we started with the set of composition-based attributes developed by Ward *et al.*[18] These attributes are primarily based on statistics of elemental properties (e.g., range in atomic radius of constituent elements), and include terms that reflect known empirical rules, such as the polydispersity of atomic radii and average number of valence electrons.[1,19] Additionally, we developed new attributes to reflect other empirical rules:

***Cluster Packing Efficiency Attributes***, which are based on the idea that bulk metallic glasses, at the atomic scale, are composed of energetically-stable arrangements that lack long-range order.[20,21] Recently, Laws *et al*. demonstrated a simple, geometric model that shows bulk metallic glasses tend to form where it is feasible for all atoms to be part of efficiently-packed clusters.[22] To integrate this knowledge, we compute the efficiently packed clusters for each system and derive attributes based on the distance between the nearest efficiently-packed clusters and the alloy composition.

***Proximity to Crystalline Compound Attributes,*** which reflect the idea that the driving force for crystallization is correlated to distance between and alloy composition and nearby crystalline compounds.[23] We represented this effect using data from the OQMD, which contains the DFT-predicted T=0 K energies of hundreds of thousands of experimentally-observed and hypothetical structures.[24,25] We compute the formation enthalpy and several measures of the distance between an alloy and the nearest phases to use as attributes.

In order to account for the sampling bias resulting in the only negative examples of glass-formation having less than 4 elements (see Training Data section), we excluded attributes that are based on the number of elements for the glass-forming ability classification model, including the "stoichiometric" attributes introduced by Ward *et al.*, and the number of crystals in equilibrium at a particular composition (i.e., due to Gibbs' Phase Rule).

A full description of these attributes and the software necessary to compute them are available in the Additional Information provided with this report. All software has also been made publically available as part of the open-source Materials-Agnostic Platform for Informatics and Exploration (Magpie).[26]

### Machine Learning Algorithms

The final ingredient of our models is a machine learning algorithm to create a function that maps the attributes in the representation to the properties of interest. In order to select the optimal

algorithm for each problem, we evaluated the performance in a 10-fold cross-validation test for over 10 different machine learning algorithms (using Weka[27]) and selected the one with the lowest Mean Absolute Error (MAE) or highest classification accuracy. The algorithm choice and cross-validation performance will be discussed in the Results section.

### Experimental Methods

All compositions were weighed out using high purity elements with at least 99.99% purity. The ingots were arc melted under a Ti-gettered argon atmosphere at least three times to ensure compositional homogeneity. They were then cast using the Engel e-motion 110 injection molding machine into a mold that consists of various rod diameters and lengths (0.8-4 mm diameter). This test specimen is given the name Strength Limiting Casting Thickness (SLCT) specimen (see Additional Material), which is designed to simultaneously evaluate the castability of an alloy and provide test samples of various diameters for mechanical testing. The SLCT specimens were then mechanically tested on a MTS 810 testing machine at a displacement rate of 15 mm/min. in bending. The fracture loads and displacements were recorded and yield strengths were calculated from these specimens. Optical micrographs of representative specimens for each rod size were obtained with a Keyence VHX-5000 digital microscope. Differential scanning calorimetry was performed with a Netzch 404C DSC at a heating rate of 20 K/min. in argon atmosphere on representative specimens to obtain $T_g$ and $T_x$.

## Results and Discussion

### Validating Machine Learning Models

We found that decision tree algorithms, specifically the Random Forest algorithm,[28] resulted in the most quantitatively accurate and predictive models in cross-validation for all three models. In the case of the $D_{max}$ and $\Delta T_x$ models, we were able to further boost the accuracy in cross-validation using the additive regression technique.[29] Full details on the selected algorithms, including metaparameter choices, are specified in the input files provided with this report.

We first validated the predictive performance of our algorithms using 10-fold cross-validation. Our classification model was found to have an accuracy of 89% and a False Positive Rate for incorrectly predicting a non-glass-forming composition as glass-forming of only 7%. We also found good predictive accuracy of our model for $D_{max}$ and $\Delta T_x$ regression models with correlation coefficients greater than 80%, as shown in Figure 2.

To study the ability of our model to extrapolate to new alloy systems, we withheld all data from the Mg-Ni-La ternary system and any derivative quaternaries to use as a test set. We chose this system in particular because the $D_{max}$ and $\Delta T_x$ for all BMGs were assessed by the same research group using the same casting technique with the same quality materials.[30,31] In this test, our regression models produced similar levels of accuracy to those reported in the cross-validation test (see Figure 3). Additionally, out of the 66 alloys in the test set, the 20 where the classification model was most confident that alloy would be glass-forming were all indeed metallic glasses. From this test, we conclude that our model is able to predict the properties of BMGs and glass-forming ability in yet-unstudied systems.

## Search for New BMG Alloys

We applied our models to two separate design tasks: identifying new alloying systems and selecting a composition that optimizes the glass-forming ability of existing alloys.

### Locating Novel Bulk Metallic Glasses

The first application we considered was using our algorithms to find alloys that are different than known BMGs and have large critical casting diameters and supercooled liquid ranges. Accordingly, we decided to evaluate alloys created using all combinations of elements out of a list of 27 suitable for commercial production using available casting techniques (see

Table **1**). From this list, we tested all combinations of two or three elements at 2 at% spacing.

*Search Strategy:* Our procedure for finding new alloys was split into four separate screens. First, we removed any alloys where the $L_1$ distance between the composition of that alloy and any known ribbon or bulk-forming glass was less than 30 at%. Next, we used the classification model to eliminate alloys that are predicted to have greater than a 5% chance of not being able to form a glass. Then, we used the regression models to locate alloys with a $\Delta T_x$ above the 80th percentile of the training data (66 K) and a $D_{max}$ greater than 1 mm.

*Search Results*: The ternary alloy search space included 3.5 million possible alloy candidates, which required about 2 days on 8, 2.2 GHz processors to complete. We first evaluated the search space using an earlier iteration of our models, which was trained on only information from the Landolt-Bornstein Handbook and Long *et al*. (2009) datasets.[13,14] Only 38361 (approximately 1%) alloys passed all of the filters. We then sorted each ternary system based on the number of alloys that passed all filters, as a proxy for the size of the glass-forming region. Out of these top alloys, we selected the Cu-Hf-Mg and Cu-Hf-Ti systems. Then, using our most-recent models, we identified alloy compositions within these system with the highest predicted $D_{max}$ and $\Delta T_x$. The top alloys we selected for testing are shown in Table 3**.**

### Tuning Established Zr-based BMG Alloys

The second application we considered was using our models to optimize the performance of two established alloys that are known to be viable with our target processing method: LM105 ($Zr_{52.5}Ti_5Cu_{17.9}Ni_{14.6}Al_{10}$) and LM601 ($Zr_{51}Cu_6Ni_{40}Al_9$). In contrast to our first design task, we constrained our search to only compositions near those of our target alloys. The search space defined for these two alloys is shown in Table 2.

From the several million possible candidates, we identified the alloys that were predicted to have the optimal balance of $D_{max}$ and $\Delta T_x$ using Pareto analysis.[32] This search required around only a few CPU-days of computer time, but would require decades to perform experimentally. As shown in Figure 4, this technique highlights alloys where no other alloy is predicted to have better performance by both metrics. In total, we identified 6 Pareto-optimal alloys for further testing, which are listed in Table 3.

### Testing Predicted Alloys

In order to evaluate the viability of our alloys in a commercial processing environment, we attempted to cast all of the alloys listed in Table 3 using arc melting and an Engel e-motion 110 injection molding machine. Of the four alloys selected from the “new system” search, we were

only able to successfully melt and cast two of the alloys. The Mg in the Cu-Hf-Mg alloys ignited during arc melting. All alloys from the tuning experiment were able to be successfully casted, though some cast worse in the Engel machine than base alloys (e.g., mold did not completely fill).

For the alloys that were able to be casted, we measured whether the alloys formed amorphous samples for a variety of rod thicknesses. To do so, we determined the Strength-Limiting Casting Thickness (SLCT), the diameter at which mechanical properties of the sample begin to degrade from the fully-amorphous behavior. For the optimization of the LM601 and LM105 alloys, we managed to achieve an SLCT comparable to the base alloys (see Figure 5), which are known to be specifically well-suited for this fabrication technique**.** Our Cu-Hf-Ti alloy did not form amorphous rods in the injection mold machine. Experiments to determine whether the inability to form a glass is an effect of inaccuracies in the machine learning model or differences between the experiments used to measure $D_{max}$ and those employed here are ongoing.

Additionally, we measured the $\Delta T_x$ of all alloys using Differential Scanning Calorimetry (DSC) and found several alloys with improved properties. For the LM601 optimization, both of our new alloys exceeded the base alloy by this performance criterion. Additionally, we also observed higher $\Delta T_x$ than the base alloy for many of the LM105 variants, also consistent with the predictions of our machine learning model. Some alloys even achieved this improved level of performance with similar casting thicknesses to the base alloys.

Overall, we were able to find several BMGs that have improved properties compared to known alloys and are able to be formed using commercial processing equipment. We have also identified other BMGs in new alloy systems that may be possible to form with different processes. From this, we conclude that machine learning searches for new alloys should be tailored for a specific fabrication process at least by limiting the search space based on knowledge about which compositions would be easiest to process or, ideally, by using data collected using the same type of process. Our success was greatest for optimizing alloys that were already known to be compatible with current processing technologies. Several of our variants of the established LM601 and LM105 alloys had larger $\Delta T_x$'s than existing alloys with similar casting thicknesses. From here, we can imagine improving our design tools by integrating other properties into the design framework and adding data from injection molding experiments to our training sets.

## Conclusions

In this report, we present a set of machine-learning-based design tools for Bulk Metallic Glasses (BMGs) and initial work on validating these predictions using commercially-viable fabrication methods. In particular, we show:

- A machine learning model to provide a link between composition and two properties of metallic glasses: critical casting thickness and supercooled liquid range
- Validation of the ability of models to extrapolate to new alloy systems
- Demonstration of using models to discover new alloys, and optimize existing BMGs

## Availability of Supporting Data

All data used to train our machine learning models was collected from publically-available literature. A full collection of the data, listing the sources, is provided along with this report.

## Tables

**Table 1.** List of elements included in search for new alloys

| ELEMENTS CONSIDERED IN ALLOY SEARCH | | | | | | |
|---|---|---|---|---|---|---|
| Mo | W | Ta | Hf | Ti | Zr | P |
| Ca | Li | Mg | Nb | Zn | Si | B |
| Co | Fe | Mn | Cr | V | Pb | C |
| Sn | In | Ag | Cu | Al | Ni | |

**Table 2.** Compositions ranges considered for each element varied for the optimization of LM105 and LM601. Between both tests, only the ranges of acceptable compositions changed and not the step sizes. All values are in at. %.

| | **LM105** | | **LM106** | | |
|---|---|---|---|---|---|
| **Element** | *Minimum* | *Maximum* | *Minimum* | *Maximum* | *Step Size* |
| Zr | 47 | 60 | 45 | 65 | 0.5 |
| Ti | 2 | 8 | 0 | 20 | 0.5 |
| Cu | 12 | 24 | 0 | 30 | 0.5 |
| Ni | 0 | 30 | 0 | 30 | 0.5 |
| Al | 5 | 15 | 0 | 20 | 0.5 |

**Table 3.** Measured and predicted properties of alloys evaluated in this work.

| | Name | Composition (at. %) | | | | | $\Delta T_x$ (K) | | SLCT (mm) | $D_{max}$ (mm) |
|---|---|---|---|---|---|---|---|---|---|---|
| | | | | | | | *Measured* | *Predicted* | *Measured* | *Predicted* |
| *LM601 Optimization* | LM601-Op1 | Zr | Cu | Ni | Al | | 96.1 | 88.8 | 2.2 | 8.8 |
| | | 48.00% | 29.50% | 4.50% | 18.00% | | | | | |
| | LM601-Op2 | Zr | Cu | Ni | Al | | 101.3 | 76.6 | 4.4 | 16.0 |
| | | 65.00% | 17.50% | 10.00% | 7.50% | | | | | |
| | LM601 | Zr | Cu | Ni | Al | | 85.0 | 81.1 | 4.3 | 6.8 |
| | | 50.75% | 36.23% | 4.03% | 9.00% | | | | | |
| *LM105 Optimization* | LM105-Op1 | Zr | Ti | Cu | Ni | Al | 83.8 | 85.5 | 3.8 | 6.5 |
| | | 55.00% | 2.00% | 23.00% | 7.50% | 12.50% | | | | |
| | LM105-Op2 | Zr | Ti | Cu | Ni | Al | 82.8 | 83.2 | 3.1 | 8.6 |
| | | 47.00% | 3.00% | 23.50% | 11.50% | 15.00% | | | | |
| | LM105-Op3 | Zr | Ti | Cu | Ni | Al | 58.8 | 76.9 | 2.4 | 9.8 |
| | | 47.00% | 2.00% | 23.00% | 18.00% | 10.00% | | | | |
| | LM105-Op4 | Zr | Ti | Cu | Ni | Al | 92.3 | 70.2 | 4.2 | 10.6 |
| | | 60.00% | 5.00% | 17.50% | 10.00% | 7.50% | | | | |
| | LM105 | Zr | Ti | Cu | Ni | Al | 68.3 | 66.5 | 4.8 | 6.4 |
| | | 52.50% | 5.00% | 17.90% | 14.60% | 10.00% | | | | |
| *Ternary Search* | CuHf-Ti ($D_{max}$) | Cu | Hf | Ti | | | *Did not form a fully-amorphous sample* | | | |
| | | 59.0% | 26.5% | 14.5% | | | | | | |
| | CuHf-Ti ($\Delta T_x$) | Cu | Hf | Ti | | | | | | |
| | | 44.00% | 45.50% | 10.50% | | | | | | |
| | CuHf-Mg ($D_{max}$) | Cu | Hf | Mg | | | *Mg ignited during melting* | | | |
| | | 35.50% | 37.50% | 27.00% | | | | | | |
| | CuHf-Mg ($\Delta T_x$) | Cu | Hf | Mg | | | | | | |
| | | 43.50% | 46.00% | 10.50% | | | | | | |

## Figures

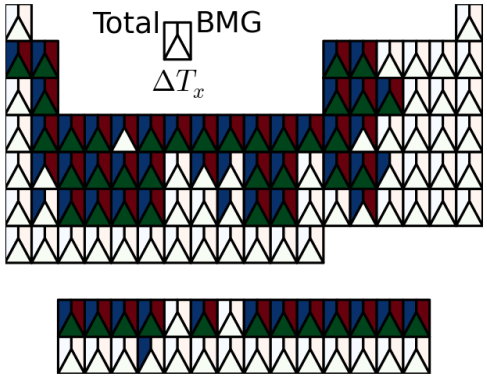


**Figure 1.** Elements present in each training dataset. The blue fill in the top left segment indicates the element is present in *any* dataset. The red fill in the top right segment indicates the element is present in BMG alloys included in our training set. The green fill on the bottom indicates the element is present in the supercooled liquid range dataset.

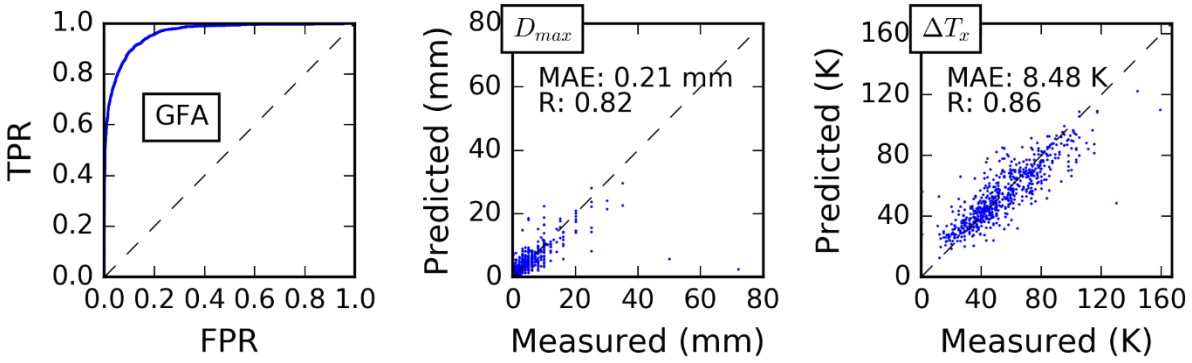


**Figure 2.** Performance of machine learning models designed to predict whether an alloy can form a metallic glass, critical casting thickness ($D_{max}$), and supercooled liquid range ($\Delta T_x$) in 10-fold cross validation. All models were tested using data taken from the metallic glass literature. The GFA classification model was characterized using a Receiver Operating Characteristic (ROC) curve, which shows the True and False Positive rates of labelling metallic glasses as a function of increasing the threshold at which an entry is labeled "glass-forming." The $D_{max}$ and $\Delta T_x$ charts show the values of the experimentally-measured properties and machine-learning-predicted values for each entry in the dataset.

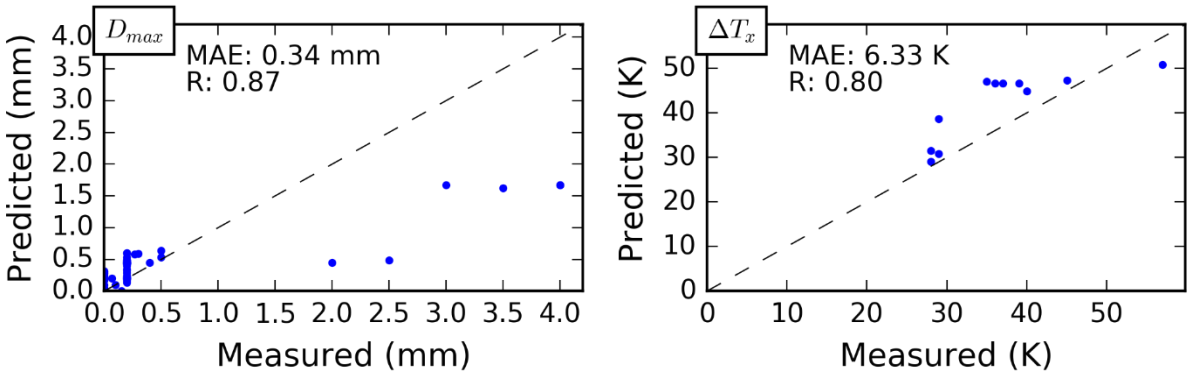


**Figure 3.** Performance of machine learning models in a test designed to evaluate their ability to extrapolate to new chemical systems. This test was performed by withholding all materials that contained exclusively Mg, Ni, and La or all three of these elements from the training data as the model, and then using the withheld entries as a test set. These charts show the measured and machine-learning-predicted values for each entry in the test set.

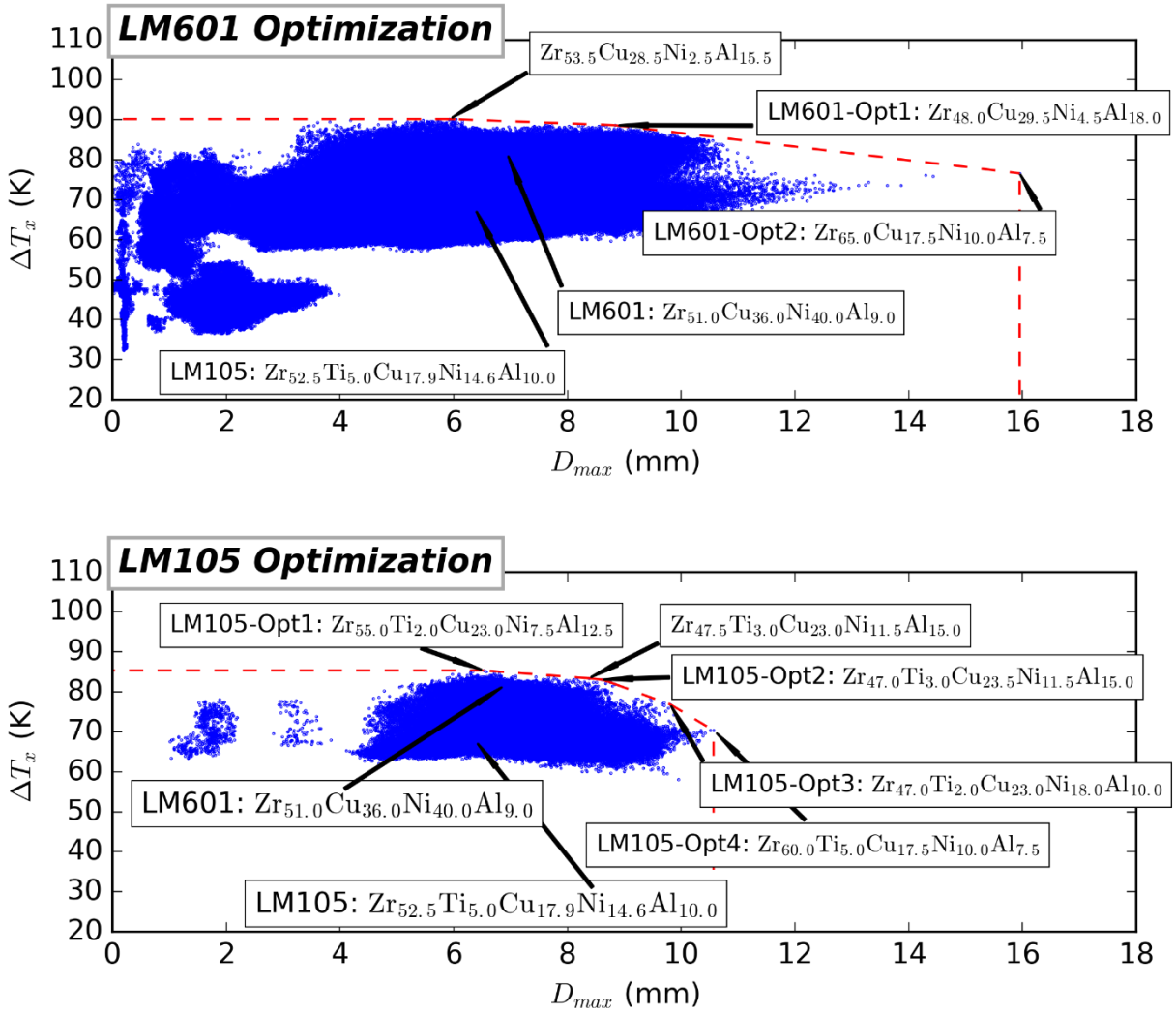


**Figure 4.** Machine-learning-predicted properties of alloys predicted during the optimization of two established BMG alloys: LM601 and LM105. The red line in each plot represents the Pareto surface of the predicted alloys, which was used to identify alloys with optimal levels of critical casting thickness ($D_{max}$) and supercooled liquid range ($\Delta T_x$). The properties, names, and compositions of alloys tested in this work are labeled with arrows.

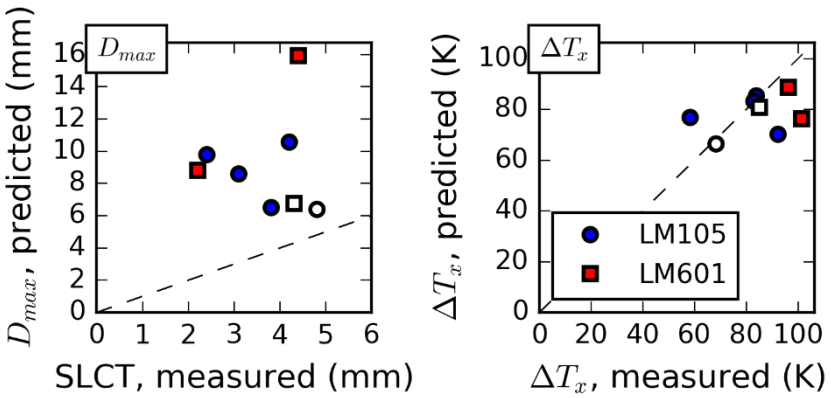


**Figure 5.** Comparison of measured and predicted values of the critical casting thicknesses and supercooled liquid ranges of alloys tested in this work. Filled points represent materials predicted by our machine learning model. Hollow points represent the base alloys. Materials with improved properties are located on the right side of each chart.

## References


1. Inoue, A. Stabilization of metallic supercooled liquid and bulk amorphous alloys. *Acta Mater.* **48,** 279–306 (2000).

2. Suryanarayana, C. & Inoue, A. *Bulk Metallic Glasses*. (CRC, 2011).

3. Yan, X. A thermodynamic approach for predicting the tendency of multicomponent metallic alloys for glass formation. *Intermetallics* **9,** 535–538 (2001).

4. Kim, D., Lee, B.-J. & Kim, N. J. Prediction of composition dependency of glass forming ability of Mg–Cu–Y alloys by thermodynamic approach. *Scr. Mater.* **52,** 969–972 (2005).

5. Gorsse, S., Orveillon, G., Senkov, O. N. & Miracle, D. B. Thermodynamic analysis of glass-forming ability in a Ca-Mg-Zn ternary alloy system. *Phys. Rev. B* **73,** 224202 (2006).

6. Ge, L. *et al.* Prediction of the glass forming ability in Cu–Zr binary and Cu–Zr–Ti ternary alloys. *Intermetallics* **16,** 27–33 (2008).

7. Kao, S.-W., Hwang, C.-C. & Chin, T.-S. Simulation of reduced glass transition temperature of Cu–Zr alloys by molecular dynamics. *J. Appl. Phys.* **105,** 064913 (2009).

8. de Oliveira, M. F., Pereira, F. S., Bolfarini, C., Kiminami, C. S. & Botta, W. J. Topological instability, average electronegativity difference and glass forming ability of amorphous alloys. *Intermetallics* **17,** 183–185 (2009).

9. Laws, K. J., Shamlaye, K. F., Wong, K., Gun, B. & Ferry, M. Prediction of Glass-Forming Compositions in Metallic Systems: Copper-Based Bulk Metallic Glasses in the Cu-Mg-Ca System. *Metall. Mater. Trans. A* **41,** 1699–1705 (2010).

10. Yang, L. *et al.* Atomic-Scale Mechanisms of the Glass-Forming Ability in Metallic Glasses. *Phys. Rev. Lett.* **109,** 105502 (2012).

11. Tang, C. & Harrowell, P. Anomalously slow crystal growth of the glass-forming alloy CuZr. *Nat. Mater.* **12,** 1–5 (2013).

12. Ding, S. *et al.* Combinatorial development of bulk metallic glasses. *Nat. Mater.* **13,** 494–500 (2014).

13. *Nonequilibrium Phase Diagrams of Ternary Amorphous Alloys*. **37A,** (Springer-Verlag, 1997).

14. Long, Z. *et al.* A new criterion for predicting the glass-forming ability of bulk metallic glasses. *J. Alloys Compd.* **475,** 207–219 (2009).

15. Tripathi, M. K., Chattopadhyay, P. P. & Ganguly, S. Multivariate analysis and classification of bulk metallic glasses using principal component analysis. *Comput. Mater. Sci.* **107,** 79–87 (2015).

16. Huang, X. M., Chang, C. T., Chang, Z. Y., Inoue, a. & Jiang, J. Z. Glass forming ability, mechanical and magnetic properties in Fe-W-Y-B alloys. *Mater. Sci. Eng. A* **527,** 1952–1956 (2010).

17. Huang, X. M. M. *et al.* Formation of bulk metallic glasses in the Fe–M–Y–B (M=transition metal) system. *J. Alloys Compd.* **460,** 708–713 (2008).

18. Ward, L., Agrawal, A., Choudhary, A. & Wolverton, C. *, submitted.* [Preprint provided in supplementary information]

19. Jiang, Q., Chi, B. Q. & Li, J. C. A valence electron concentration criterion for glass-formation ability of metallic liquids. *Appl. Phys. Lett.* **82,** 2984 (2003).

20. Miracle, D. B. A structural model for metallic glasses. *Nat. Mater.* **3,** 697–702 (2004).

21. Sheng, H. W., Luo, W. K., Alamgir, F. M., Bai, J. M. & Ma, E. Atomic packing and short-to-medium-range order in metallic glasses. *Nature* **439,** 419–25 (2006).

22. Laws, K. J., Miracle, D. B. & Ferry, M. A predictive structural model for bulk metallic glasses. *Nat. Commun.* **6,** 8123 (2015).

23. Falcão de Oliveira, M. A simple criterion to predict the glass forming ability of metallic alloys. *J. Appl. Phys.* **111,** 023509 (2012).

24. Kirklin, S. *et al.* The Open Quantum Materials Database (OQMD): assessing the accuracy of DFT formation energies. *npj Comput. Mater.* **1,** 15010 (2015).

25. Saal, J. E., Kirklin, S., Aykol, M., Meredig, B. & Wolverton, C. Materials Design and Discovery with High-Throughput Density Functional Theory: The Open Quantum Materials Database (OQMD). *Jom* **65,** 1501–1509 (2013).

26. http://bitbucket.org/wolverton/magpie

27. Hall, M. *et al.* The WEKA data mining software. *ACM SIGKDD Explor. Newsl.* **11,** 10 (2009).

28. Breiman, L. Random forest. *Mach. Learn.* **45,** 1–35 (1999).

29. Friedman, J. H. Stochastic gradient boosting. *Comput. Stat. Data Anal.* **38,** 367–378 (2002).

30. González, S. *et al.* Effect of mischmetal substitution on the glass-forming ability of Mg–Ni–La bulk metallic glasses. *Intermetallics* **17,** 968–971 (2009).

31. González, S., Figueroa, I. A. & Todd, I. Influence of minor alloying additions on the glass-forming ability of Mg–Ni–La bulk metallic glasses. *J. Alloys Compd.* **484,** 612–618 (2009).

32. Lejaeghere, K., Cottenier, S. & Van Speybroeck, V. Ranking the Stars: A Refined Pareto Approach to Computational Materials Design. *Phys. Rev. Lett.* **111,** 075501 (2013).